Triggered Fault Slip by the 2017 Mw 7.3 Iran-Iraq Earthquake

Bennett Kellmayer
GEOL394
Advisor: Dr. Mong-Han Huang

DEPARTMENT OF GEOLOGY
UNIVERSITY OF MARYLAND
COLLEGE OF COMPUTER, MATHEMATICAL, & NATURAL SCIENCES
DEPARTMENT OF GEOLOGY

Introduction

Earthquakes are a well-known hazard to people living in seismically active areas of the world. However, new evidence suggests that earthquakes can trigger fault slip and possibly generate more and smaller earthquakes to occur at distance. This is because of the release of energy and the increase of dynamic or static Coulomb stress on the receiver faults can potentially trigger these faults to slip. In this study, interferometric synthetic aperture radar (InSAR) is used to investigate shallow slip on faults that are likely to be triggered by the 2017 Mw 7.3 Iran-Iraq earthquake was investigated.

Figure 1: Study Area
Map of earthquake region from ESRI. The epicenter is marked with a yellow star and the major plate boundaries are marked with red lines.[1]

Hypothesis

Null: There was no discernable connection between the Coulomb stress change of the region as a result of the 2017 Mw 7.3 Iran-Iraq earthquake and the triggered slip.
Alternative One: There is a discernable connection between the static Coulomb stress change of the main shock and the triggered slip.
Alternative Two: There is a discernable connection between the dynamic Coulomb stress change of the main shock and the triggered slip.

Methods

To explore these hypotheses further the static Coulomb stress change was calculated and plotted spatially against the triggered slip events. To examine the dynamic coulomb stress change as a result of the main shock, the propagation of the earthquake was modeled using finite fault inversion and synthetic seismograms.

Figure 2: InSAR Observations
Coseismic interferogram of the 2017 Mw 7.3 Iran-Iraq Earthquake with notable surface deformation marked with black lines. Epicenter location denoted with yellow star.

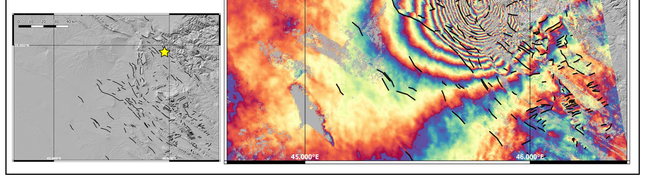

Background

Figure 3: Earthquake Directivity
- Faults rupture propagates forward in a given direction based on the orientation of the fault plane
- The area this propagation would pass through if not arrested receives a dynamically higher seismic wave signal
- Though temporary this dynamic signal can alter fault properties and allow for triggered slip

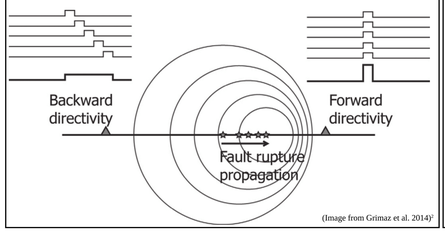

(Image from Grimaz et al. 2014)[2]

Figure 4: Coulomb Stress Criterion
- Proxy for ground stability
- Failure occurs when $\Delta\sigma_f$ exceeds a value given by:
- $\Delta\sigma_f = \Delta\tau_\beta - \mu(\Delta\sigma_\beta - p)$
- $\Delta\sigma_f$ = Coulomb stress change
- $\Delta\tau_\beta$ = change in shear stress
- $\Delta\sigma_\beta$ = change in normal stress
- p = pore fluid pressure
- μ = the coefficient of friction

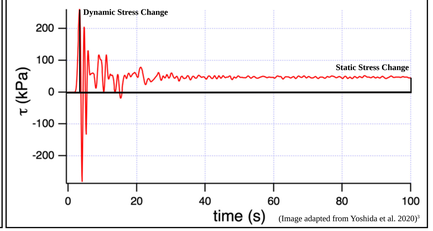

(Image adapted from Yoshida et al. 2020)[3]

Results

Figure 5: Seismic Moment Distribution
- 900 subfaults
- Incorporates seismic moment distribution on the fault plane from USGS
- Maximum Mo = 2.39e+18 dyne/cm2
- Map is along the fault plane
- Hypocenter denoted with white star
- Strike: 354°
- Dip: 16°
- Depth: 15 km

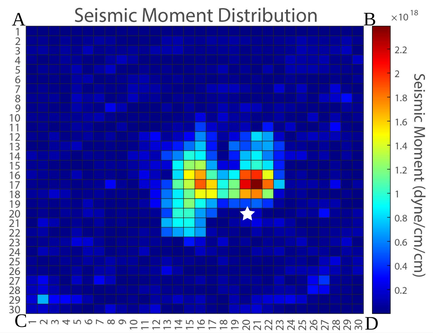

Figure 6: Static Coulomb Stress Change Inversion
- Shown here is the maximum static Coulomb stress change imposed by the earthquake
- Observed slip areas were found primarily in statically strengthened area
- Data sourced from USGS and calculated over an east dipping fault plane with 900 sub faults
- Strike: 60°
- Dip: 85°
- Rake: 180°
- Modeled using Coulomb 3.3 from USGS[4]

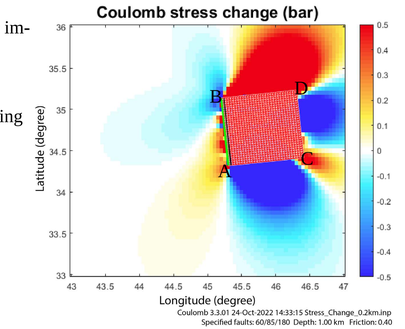

Summary

The findings of this study have implications about the nature of triggered fault slips occurring from the main shock of an earthquake system. The clear directivity shown by the simulations is quite well spatially correlated with the areas of observed slip. This coupling of directivity and surface expression is quite telling for how earthquakes nucleate and propagate as they rupture. However, there were also some slip events that were observed outside of this zone of high dynamic Coulomb stress change, indicating that this triggering mechanism is likely not responsible for every slip seen with InSAR. This pattern of slip triggering can likely be observed in other earthquake systems and future studies will be beneficial to compare the dynamic triggering of this event with other earthquake systems.

Results

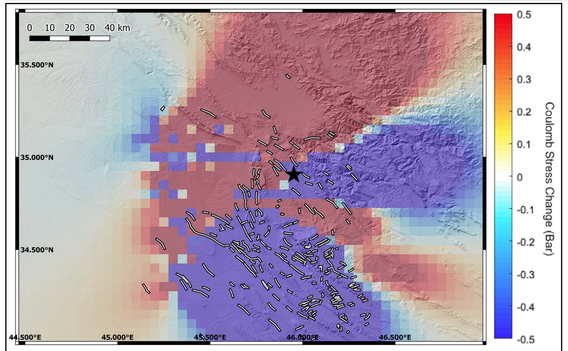

Figure 7: Static Coulomb Stress Compared to Observed Fractures
- Observed triggered slips marked with black and white lines, and the epicenter is marked with a black star.
- Static Coulomb stress change map from the Coulomb 3.3 software was mapped onto the map of fractures using QGIS.
- The location of the slip pattern in question is inconsistent with the first alternative hypothesis since the region in which the fractures are located was statically strengthened by the earthquake.
- Therefore, it is very unlikely that these fractures are due to the static stress change of the earthquake

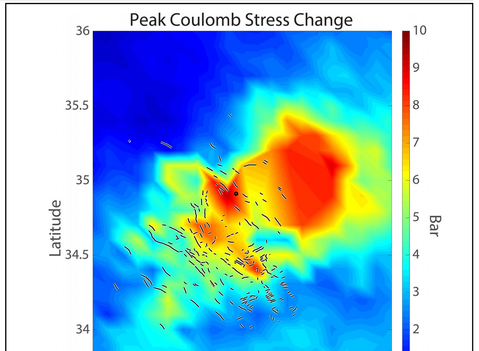

Figure 8: Peak Coulomb Stress Change
- Observed triggered slips marked with black and white lines, and the epicenter is marked with a black circle. Stress calculations measured in Pascal.
- Better spatial correlation of observed triggered slip with peak Coulomb Stress Change.

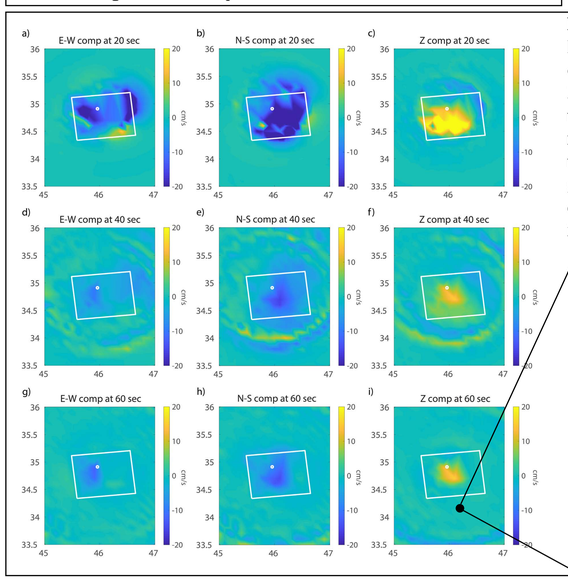

Figure 9: Three-Component Velocity Propagation
Images taken from an animation depicting the three-component velocity as it propagates through the system at 20, 40, and 60 seconds after the main shock. In each subplot the vertical axis represents latitude, the horizontal axis represents longitude, and the color bar ranges from -20 cm/s to 20 cm/s. For the purposes of this figure subplots a, d, and g depict east as positive. Similarly, subplots b, e, and h depict north as positive. Finally, subplots c, f, and i depict increasing altitude as positive.

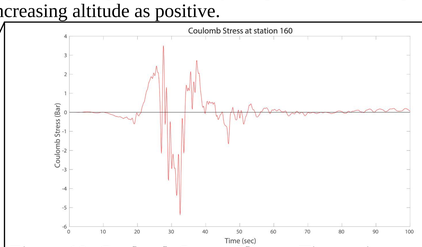

Figure 10: Coulomb Stress Change Timeseries
Simulated timeseries of Coulomb stress change at station 160, which corresponds to 34.2 degrees lattitude by 46.2 degrees longitude. Station location is marked with a black circle on Figure 9i.

Acknowledgements

- I would like to thank Dr. Mong-Han Huang for being an amazing mentor to me throughout this process.
- I would also like to thank all of the members of the Active Tectonics Laboratory, who welcomed me into their space and helped me.
- Finally, I would like to thank Dr. Phillip Piccoli for coordinating the senior thesis program in the department.

References

1: ESRI. (2011). *National Geographic World Map* [Map]. ESRI. https://www.arcgis.com/home/item.html?id=b9b1b422198944fbbd5250b3241691b6
2: Grimaz, S., & Malisan, P. (2014). *Near Field Domain Effects and Their Consideration in the International and Italian Seismic Codes*. https://doi.org/10.4430/bgta0130
3: Yoshida, S., Maeda, T., & Kato, N. (2020). Earthquake triggering model based on normal-stress-dependent Nagata law: Application to the 2016 Mie offshore earthquake. Earth, Planets and Space, 72(1), 141. https://doi.org/10.1186/s40623-020-01272-5
4: Toda, S., Stein, R.S., Sevilgen, V., and Lin, J., (2011), Coulomb 3.3 Graphic-rich deformation and stress-change software for earthquake, tectonic, and volcano research and teaching—user guide: U.S. Geological Survey Open-File Report 2011–1060, 63 p., available at https://pubs.usgs.gov/of/2011/1060/.